Journal of Advances in Computer Research
Quarterly pISSN: 2345-606x eISSN: 2345-6078
Sari Branch, Islamic Azad University, Sari, I.R.Iran
(Vol. 8, No. 1, February 2017), Pages: 89-105
www.jacr.iausari.ac.ir

A New IRIS Segmentation Method Based on Sparse Representation

Mohammad Rajabi[1], Sedigheh Ghofrani✉[1] and Ahmad Ayatollahi[2]

1) Electrical and Electronic Engineering Department, Islamic Azad University, South Tehran Branch, Tehran, Iran
2) Electrical Engineering Department, Iran University of Science and Technology, Tehran, Iran

m.rajabi08@gmail.com; s_ghofrani@azad.ac.ir; ayatollahi@iust.ac.ir

Received: 2016/06/09; Accepted: 2016/07/18

Abstract

Iris recognition is one of the most reliable methods for identification. In general, it consists of image acquisition, iris segmentation, feature extraction and matching. Among them, iris segmentation has an important role on the performance of any iris recognition system. Eyes nonlinear movement, occlusion, and specular reflection are main challenges for any iris segmentation method. In this paper, we propose a new pupil localization method based on the sparse representation and sparse recovery (SR). The main advantage of our segmentation algorithm based on sparse representation in respect to other approaches is capability of searching the whole image for iris region very fast. Also we have proposed a new method for enhancing the extracted iris template when the pupil boundary is noncircular, and also a new method for creating occlusion mask based on the histogram thresholding. We have compared the SR classifier and the Hamming distance (HD) with the same size dictionary and shown that using the principal component analysis (PCA) with the SR classifier makes it very faster, whereas preserves the accuracy. The achieved results are evaluated with others in terms of the recognition accuracy and the segmentation time consuming where the CASIA V4 Lamp database used.

Keywords: *Iris Segmentation and Recognition, Sparse Representation, Eyelid and Eyelash Detection, Principal Component Analysis.*

1. Introduction

Iris is a part of human eye that is between the black pupil and white sclera. Human iris has a rich texture structure and is also unique and stable in the whole life duration for individuals [1]. In addition, iris acquisition is contactless and this property is important where a personal identity in high privacy place is to be checked. So, the human iris recognition is one of the most attractive biometric methods.

The task of iris segmentation stage is localizing the iris region. There are many methods for iris segmentation, among them, some only find the iris inner and outer boundaries, others also detect the eyelids and eyelashes and try to remove their signs [2], [3]. Two pioneer methods for iris segmentation were introduced by Daugman [4] and Wildes [5]. Both approaches are based on considering the iris boundary as a circle shape. Daugman considered the Integro-differential operator that first smooths the image by Gaussian low pass filter and then searches for the maximum angular integral

of the radial derivative over the image domain. Wildes localized the iris boundaries by edge detection which followed by the circular Hough transform.

At the beginning, the most researchers [6], [7], [23] focused on improving Daugman [4] and Wildes [5] methods. In [6], the combination of the Integro–differential operators using Hough transform was proposed for iris segmentation. In [23], the wide range iris segmentation algorithms were reviewed and the circular Hough transform was optimized. Although, in recent years, the iris boundaries were segmented based on different models such as Geodesic active contours [8], Fourier series expansions [2] and pulling pushing method [3], some researchers worked on detecting and removing the occlusion [9], [10] caused by eyelid and eyelash to improve the accuracy of iris recognition system.

In this paper we propose a new method based on sparse representation where the inner iris boundary is found in gradient domain. We find the pupil boundary by proposing the sparse pupil localization (SPL) method and then extract the data around the pupil with desired radius. Our new iris segmentation method, shown in Fig. 1, consists of three stages; preprocessing (which includes removing reflections and detecting edges), localizing pupil and normalizing iris. After normalizing the iris region, we try to reduce the noncircular effect of the pupil boundary by using the template column circular shift (TCCS). Then, we extract features of the iris template by using wavelet transform. Finally, we propose a method based on thresholding histogram named histogram eyelid eyelash detector (HEED) that can simultaneously reduce or remove the effect of eyelids and eyelashes in the extracted template. At the end, we evaluate the performance of our proposed method by using HD, SR classifier and combination of PCA and SR classifier on the CASIA V4.0 Lamp iris database. In addition, the performance of our method is compared with others in terms of time consuming and recognition accuracy.

Our proposed approach in spite of its rich scientific background is implemented easily, and with simple preprocessing can get convenient results. Specifically, the pupil boundary enhancement algorithm can be applied for any iris recognition system using the Daugman Rubber Sheet method and increase the recognition rate. The implementation of our algorithm to detect the eyelids and eyelashes only needs the extracted template image histogram and does not need any curve fitting. The achieved accuracy of our proposed method in comparison with two recently published papers [3], [22] is appropriate and the computation cost is efficient.

The paper is organized as follows. The sparse representation and SR theory are explained in Section 2. The proposed method including reflection removal, pupil localization, normalization, eyelid and eyelash detection, and the classification is expressed in Section 3. The experimental results are given in Section 4 and finally Section 5 is the paper conclusion.

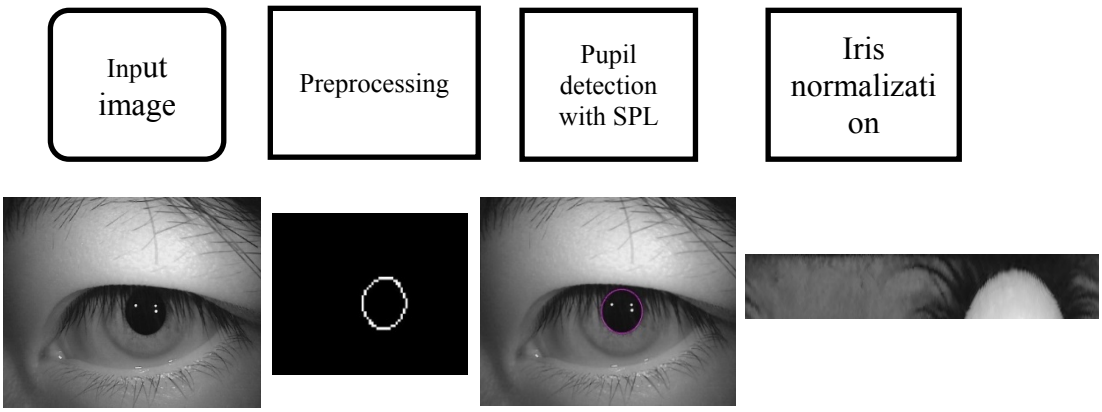

Fig. 1: Block diagram of the proposed segmentation method.

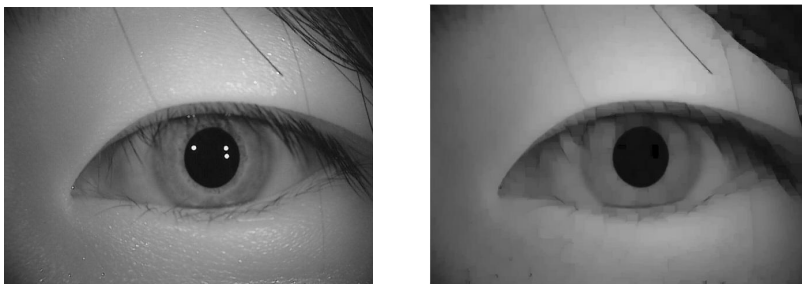

(a) (b)

Fig. 2: (a) The original input image, (b) using the morphological opening function removes the specular reflection.

2. Sparsity and Compressibility

Many natural signals have concise representations when expressed by suitable basis. It means that if a signal has only few large nonzero values in some basis, it can be recovered by discarding small coefficients without perceptual loss. From a general point of view, sparsity and more generally, compressibility has a fundamental role in many fields of science. Sparsity leads to efficient estimations; for example, the quality of estimation by thresholding or shrinkage algorithms depends on the sparsity of the signal we wish to estimate. Sparsity also leads to efficient compression; for instance, the precision of a transform coder depends on the sparsity of the signal we wish to encode [11].

In recent years researchers have paid more attention to the sparse representation and sparse recovery. Due to, Wright et al. [12] introduced a sparse representation-based face recognition algorithm, which outperforms many state-of-the-art algorithms when a sufficient number of training images are available and Pillai et al. [13] proposed secure iris recognition method based on the random projections and sparse representations.

2.1 Sparse Representation and Sparse Recovery

In signal processing field, a signal is sparse or approximately sparse if it only has few nonzero elements or it has few large elements and others are almost equal to zero. Also, some signals such as sinusoids are not sparse at their original domain where as they may be sparse if they are expressed by an appropriate basis (i.e. the sinusoid is not sparse in time domain but it is completely sparse in frequency domain). So, finding the sparse

basis and defining the sparse domain is the main challenge of using the benefit of the sparse representation or SR. Many researchers in different fields like mathematics, computer science and statics are working on the SR methods and its applications [14], [15].

In general, any observed signal, y(t), can be written in some basis (like Fourier, wavelet, discrete cosine transform, and Dirac delta) as:

$$y(t) = \sum_{i=0}^{N-1} x_i a_{i,t} \tag{1}$$

Where $t = 0,..., M-1$ refers to the different observation time, x_i is the element of coefficient vector $\mathbf{x}$ and $a_{i,t}$ denotes the elements of basis dictionary $\mathbf{A}$. Easily, Eq. (1) can be written in matrix form as:

$$\mathbf{y} = \mathbf{A}\mathbf{x} \tag{2}$$

Where $\mathbf{y} = [\, y(t_0),\, y(t_1),...,\, y(t_{M-1})]^T$, $\mathbf{A} = [\mathbf{a}_0, \mathbf{a}_1, ..., \mathbf{a}_t, ..., \mathbf{a}_{N-1}]$, $\mathbf{a}_t = [a_{0,t}, a_{1,t}, ..., a_{M-1,t}]^T$, $\mathbf{x} = [\, x_0,\, x_1, ...,\, x_{N-1}]^T$ and $(.)^T$ denotes the transpose. For under-sampled measurements or under-determined problem where $M \ll N$, Eq. (2) does not have unique solution. In this case, the SR theory is able to find the coefficient vector **x**. It has been shown that if **x** is sparse enough [11] and **A** has specific conditions, the sparsest **x** can be recovered by solving the following optimization problem:

$$\text{minimize } \| \hat{\mathbf{x}} \|_{\ell_1} \qquad \text{subject to} \qquad \mathbf{y} = \mathbf{A}\hat{\mathbf{x}} \tag{3}$$

Often, the observed vector includes some noise, so it is modeled as:

$$\mathbf{y} = \mathbf{A}\mathbf{x} + \mathbf{e} \tag{4}$$

Where $\mathbf{e}$ is stochastic or deterministic error term with bounded energy $\| \mathbf{e} \|_{\ell_2} < \varepsilon$. Then, the sparsest **x** is obtained by solving the following problem:

$$\text{minimize } \| \hat{\mathbf{x}} \|_{\ell_1} \qquad \text{subject to} \qquad \| \mathbf{A}\hat{\mathbf{x}} - \mathbf{y} \|_{\ell_2} < \varepsilon \tag{5}$$

These are convex optimization problems which can be recast into a linear program.

3. The Proposed Method

The proposed method as shown in Fig. 1 consisting three stages in general where every stage may include different sub-systems explained in the following.

3.1 Reflection Removal and Edge Detection

In order to reduce the computation cost, the image resizing is done before performing the reflection removal algorithm, where the aspect ratio of input and output image is equal to six. In addition, if the image size is too big with useless background, it should be cropped before resizing. Fig. 2-a shows a sample image with existence the high intensity reflections located on the pupil. Therefore, they look like bright holes on the dark area. The morphological opening and closing function is used sequentially to fill these white holes as shown in Fig. 2-b. After removing the eye reflections, the grayscale iris image is converted to binary by considering the threshold value T. The optimum threshold value depends on the image acquisition procedure or image capturing condition. Therefore, the threshold value can be generally pre-defined for a data set or it can be determined for every image adaptively,

$$T = m + c \tag{6}$$

Where m refers to the minimum intensity value of image and c is a constant determined according to the data set. After binarization, the edges are detected by using the Sobel gradient operator. In this way, the preprocessing finishes and the pupil region is found as explained in following.

3.2 Pupil Localization with Sparse Recovery

The main challenges for any iris recognition system are finding the pupil boundary and extracting the iris texture data correctly. The novelty of this paper is using the SR algorithm for finding the pupil boundary. For this purpose, the over complete dictionary including circles with different radius and centers is generated to cover the all coordinate of an image. If we consider the vectorized output image of Section 3.1 as $\mathbf{y}$ and the generated dictionary consisting different circles as $\mathbf{A}$, then the pupil localization, considering in Section 2.1 is modeled as follows,

$$\mathbf{y} = \mathbf{A}\mathbf{x} + \mathbf{e} \tag{7}$$

Where $\mathbf{x}$ is the sparse coefficients vector whose nonzero values refer to the candidate circles in the dictionary and the undesired detected edges are modeled as an error, $\mathbf{e}$. Eq. (7) is inherently under-determined because the number of generated circles is greater than the size of preprocessed image. Furthermore, there is the sparse solution for this problem because only one circle matches on the pupil boundary. The procedures of generating the dictionary $\mathbf{A}$ is shown in Fig. 3.

By solving Eq. (7) using the SR algorithms, the desired index (where the largest value of $\mathbf{x}$ is located) of the vector $\mathbf{x}$ corresponding to a circle in the dictionary $\mathbf{A}$ is obtained. It means the desired index of $\mathbf{x}$ by considering the dictionary $\mathbf{A}$ shows the circle characteristic (radius and center coordinate) that matches to the pupil boundary.

There are many algorithms for solving ℓ_1 norm minimization problems such as primal dual interior points [19], gradient projection [20] and Homotopy [16]. In this paper, the Homotopty algorithm is used because it is fast and accurate and under specific circumstance it needs only k iterations for a k-sparse signal. In our problem, all coefficients of vector $\mathbf{x}$ except one are exactly or approximately equal to zero. Therefore, employing Homotopy algorithm recovers the vector $\mathbf{x}$ after one iteration. In this way, the SR not only is used for detecting the pupil boundary but also the computation cost is efficiently low by choosing the suitable recovery algorithm. We named this method as sparse pupil localization (SPL). In this work, the CASIA V.4 Lamp database is used and Fig. 4 shows that the segmentation based on SR is working properly even for difficult cases.

3.3 Normalization and Dealing with Noncircular Pupils

The iris texture data should be extracted after finding a pupil boundary. It is known that the texture near the pupil (Collarette area) is richer than the iris texture far from the pupil, but simply capturing the iris texture data near the pupil boundary by considering a constant offset from the pupil radius [18] is not always convenient. For any individuals, the size of pupil is varying by lighting conditions whereas the size of iris outer boundary is not changing at all.

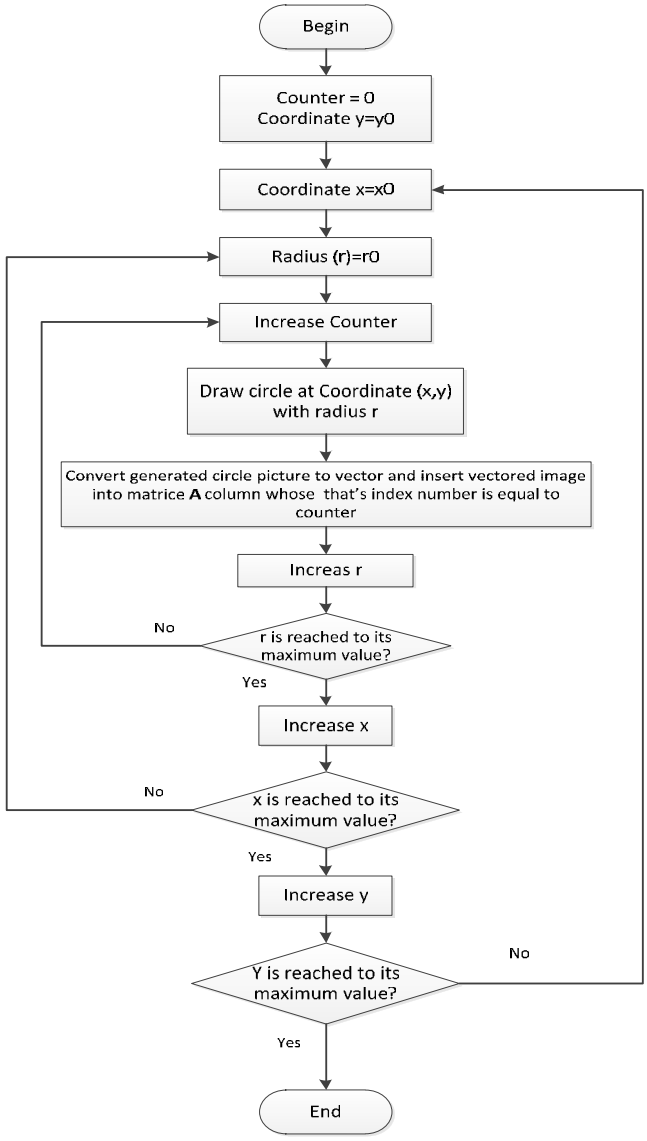

Fig. 3: The procedure of generating a redundant dictionary including circles with different center coordinate and radius.

If we assume that the distance between camera and person is fixed, then, the iris size of individuals is supposed to be a constant value. So, assuming the variable pupil size under different illumination condition and choosing a constant radius for iris, really compensate the variation size of iris (by taking the same iris area for each class) and leads to proper iris area normalization in the extracted templates. According to the images size (640×480 pixels) of CASIA V4 Lamp, the whole iris ranges are between 60-120 pixels. So, in this paper, in order to reduce the computation cost, the constant value for the radius of 90 pixels was chosen instead of finding the exact iris boundary.

Therefore, we have always used the information of Collarette area for any extracted template. It should be noted that this assumption is not only usable for CASIA V4 Lamp but also applicable for all captured images with OKI IRISPASS-h (the camera model name that captured the images of CASIA V4 Lamp) or similar devices with the same resolution such as IKEMB-100 and CASIA-IrisCamV2 camera and the same distance between camera and eye, see Fig. 5 and Fig. 6.

Fig. 4: Shown the pupil localizing by using the SPL.

According to the inner radius obtained by SPL and considered outer radius of iris, the data is extracted and normalized by using Daugman Rubber Sheet model [17]. As our segmentation method is circle based, which it finds the pupil boundary as a circle shape in iris image, so the segmentation method cannot detect the pupil boundary well in some cases such as different illumination conditions or angled images that pupil is deformed to elliptical shape, Fig. 7-a and Fig. 7-b.

To compensate the noncircular pupil boundary, in this paper, we propose TCCS method. As TCCS works on the extracted template, it can be applied to any iris recognition algorithm that uses Daugman Rubber Sheet model for normalization the iris area. In addition, it improves recognition rate by enhancing the detected pupil radius in different regions of iris template. For doing this, we assume the radius of pupil 10 pixel less than the determined value. According to CASIA V4 Lamp images, 10 pixels is the maximum possible distortion for the pupil boundary. In some cases where pupil has not a circle shape, considering the exact obtained radius causes missing a portion of useful iris data. By looking at the extracted template data shown in Fig. 7(a1, b1), top to bottom, it is seen that the most intensity variation occurs among borders of the iris and pupil. The goal is converting the curve shape border into straight line. So, at first, the effects of probable reflections on pupil area is removed by using the morphological opening function, then the effects of undesired edges on the template is reduced by using an averaging filter. Now, the edge border curve between pupil and iris is obtained by using the canny edge detector, which is the first detected edge in each column from top to bottom. Then, by using the local regression methods, we smooth the extracted data of this border.

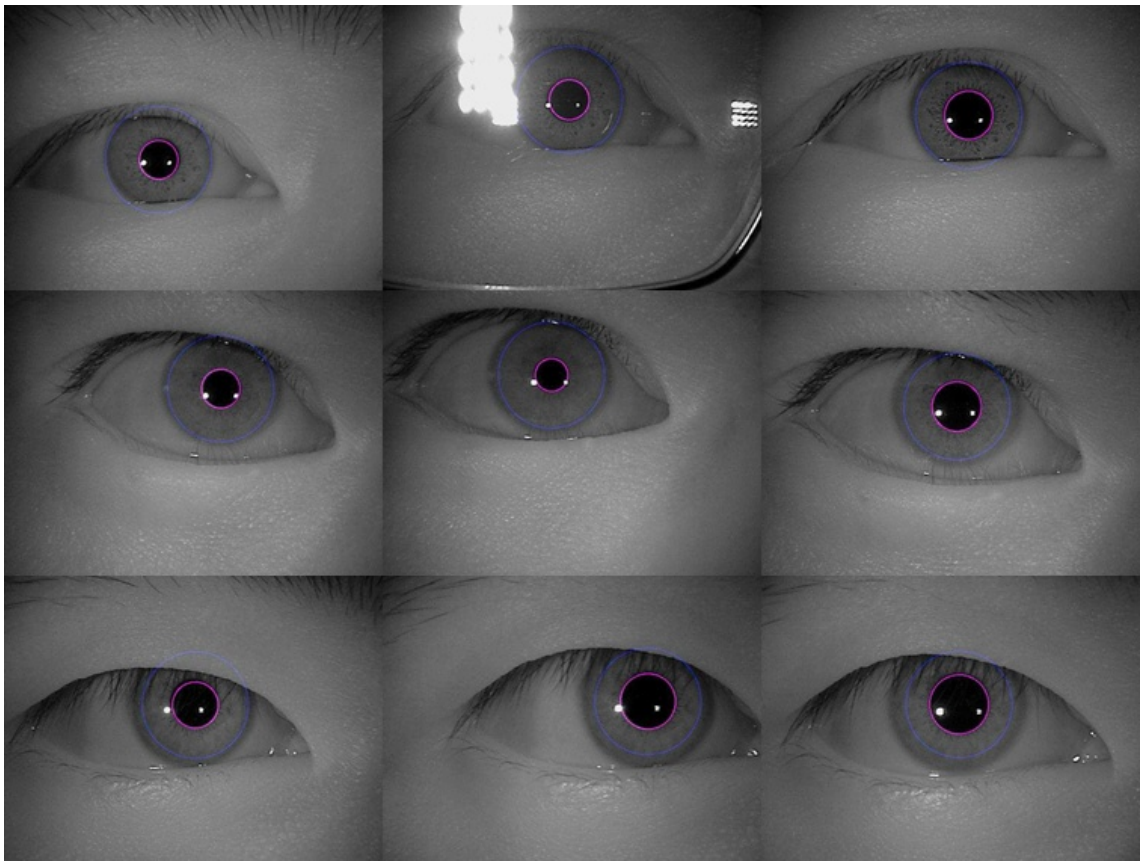

Fig. 5: The iris segmentation of the proposed method for sample images belonging to CASIA V4.0 Thousand which captured by IKEMB-100 camera. The first row are S5000L00, S5000L04, S5000L08, the second row are S5005L01, S5005L03, S5005L09 and the third row are S5007L01, S5007L04, S5007L08. The purple colored circle is pupil detection result and the blue colored circle is a fixed radius (90 pixel).

Having this information, every column of a template can be shifted up until the detected border in each column reach the first row, Fig. 7(a2, b2). At the end, the last 10 rows of template corresponding to consider the 10 pixels extra are discarded, Fig. 7(a3, b3).

3.4 Eyelid and Eyelash Detection

Eyelid and eyelash are two occlusion sources that may degrade the performance of iris recognition system. Some researchers tried to detect eyelid and eyelash in an iris image after localizing the pupil by using the curve fitting algorithm [4], [5] whereas others took afford to detect the eyelid and eyelash in the extracted template [24]. In [24], two stages named the parabolic Hough and the Otsu's thresholding were proposed for the eyelid and eyelash detection in a normalized iris image.

In this paper, a new and computationally efficient method based on thresholding histogram is proposed. The algorithm is discarding not only the eyelid and eyelash but also the shadow and reflections of the extracted iris template, in addition, it is applicable for any system working based on Daugman Rubber Sheet model.

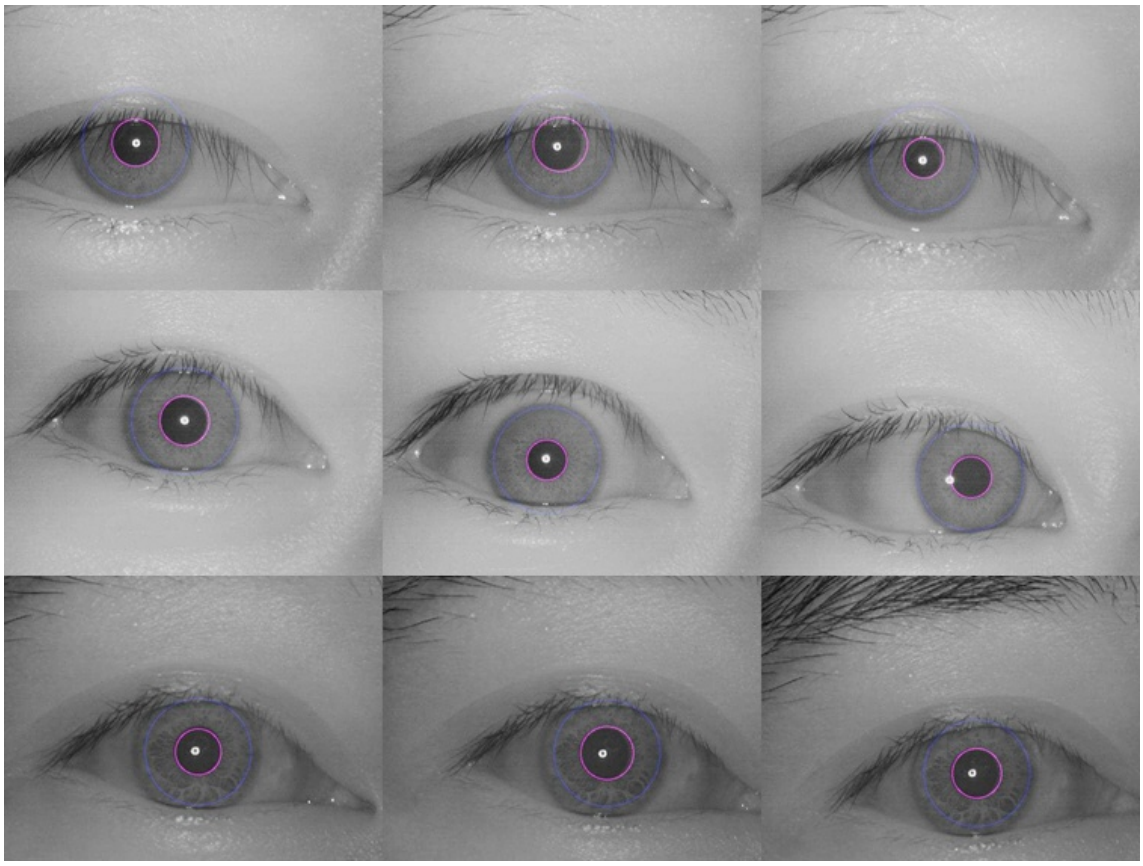

Fig. 6: The iris segmentation of the proposed method for sample images belonging to CASIA V2.0 which captured by CASIA-IrisCamV2. The first row are 0000_000, 0000_003, 0000_016, the second row are 0002_000, 0002_008, 0002_012 and the third row are 0006_000, 0006_007, 0006_015. The purple colored circle is pupil detection result and the blue colored circle is a fixed radius (90 pixel).

Clearly, by looking at the extracted iris template in Fig. 7, the template consists of three intensity tones; dark for eyelashes, medium for iris texture and bright for eyelid and reflections. Furthermore, iris occupies the largest area in a template, so we expect the histogram of any template has a peak value of medium intensity which belongs to the iris texture. We have shown this property in Fig. 8-a by averaging the histograms of all extracted templates from CASIA V4.0 Lamp left eye.

Now, the upper- and lower- threshold values for any template are obtaining in order to remove the eyelash and eyelids data. As mentioned above, iris has medium intensity in comparison with eyelid and eyelash and occupies the largest area in any template, so, in a normalized histogram, the average intensity is to be near the peak value. In this way, finding the eyelash and eyelid area is equivalent to estimate the iris intensity range for a template histogram. For this purpose, the average intensity of each template is assumed to be the length of band-pass filter. In order to distinguish the iris area from the eyelash and eyelids, the lower- and upper- thresholds (T_l , T_u) are obtained as,

$$T_l = I_{\max} - (\frac{N_l}{N_t}) I_{\text{avg}} \tag{8}$$

$$T_u = I_{\max} + (\frac{N_h}{N_t}) I_{\text{avg}} \tag{9}$$

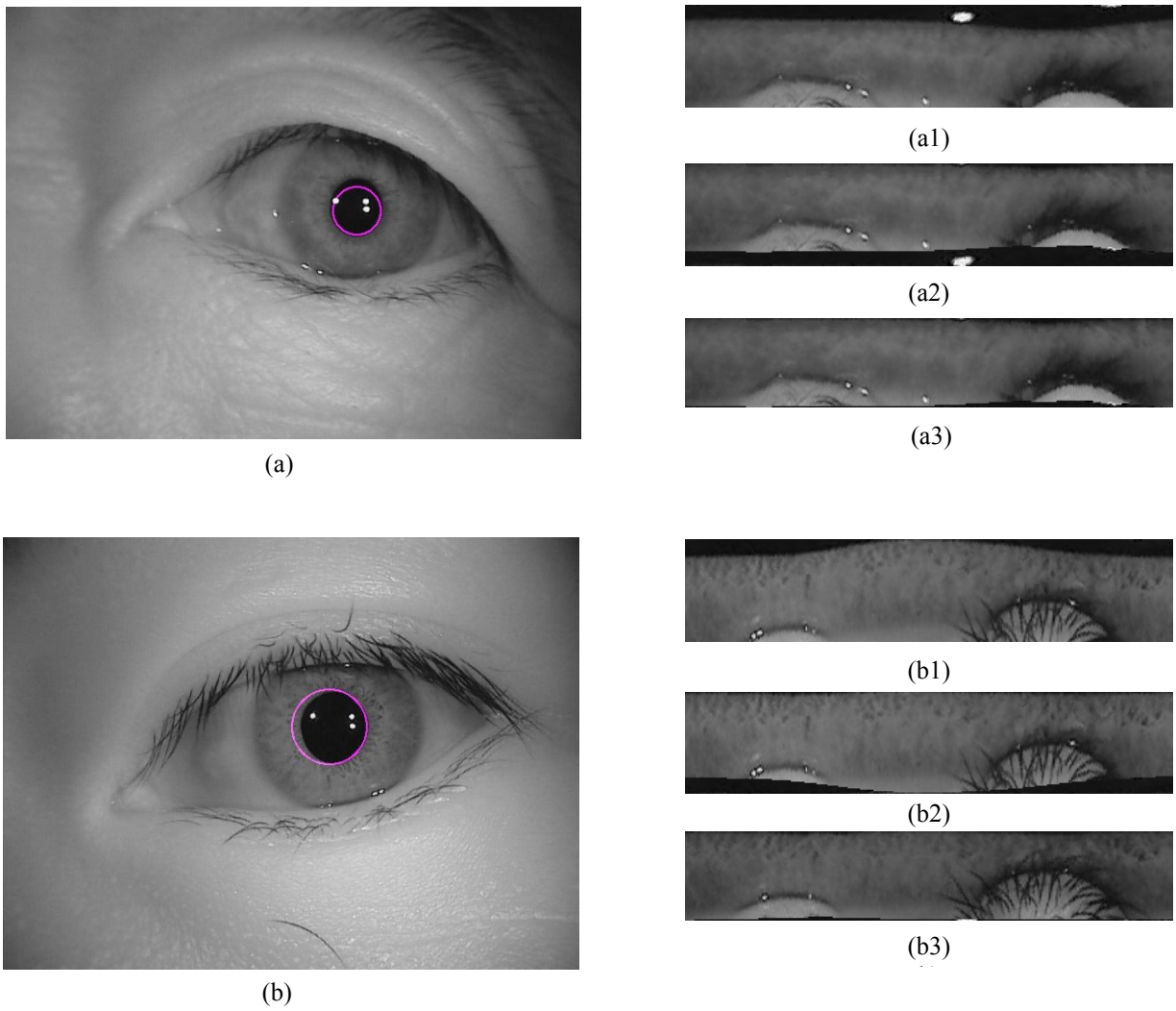

Fig. 7: (a), (b) Two samples iris images of CASIA V4.0 Lamp, specifically 318L18 and 14L15, and the obtained circle for segmenting the inner iris boundary; (a1), (b1) the extracted iris data by using Daugman Rubber Sheet; (a2), (b2) shifted version by the proposed method; (a3), (b3) cropped template where there is no useless information any more.

Where $I_{\max}$ refers to the intensity value with maximum number of pixels (histogram peak), N_l and N_h are the number of pixels whose intensities are less and greater than $I_{\max}$, N_t is the total number of pixels in a template, and I_{avg} denotes to the mean intensity value of the template which is also the band-width of the band-pass filter (i.e. $T_u - T_l = I_{\text{avg}}$). A sample histogram and the obtained thresholds are shown in Fig. 8-b.

In this way, according to the normalized histogram and obtained thresholds, a binary mask for each template is built up. The binary mask of a template is used for classification by HD. Sample generated binary masks are shown in Fig. 9.

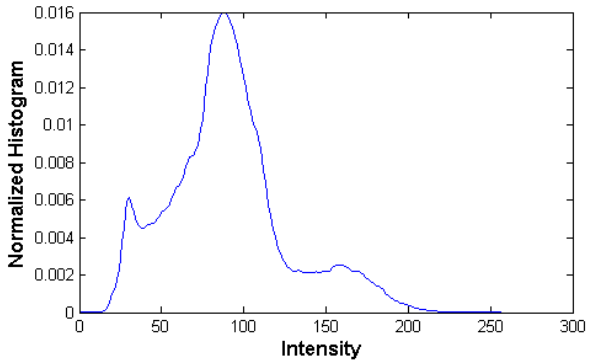

(a)

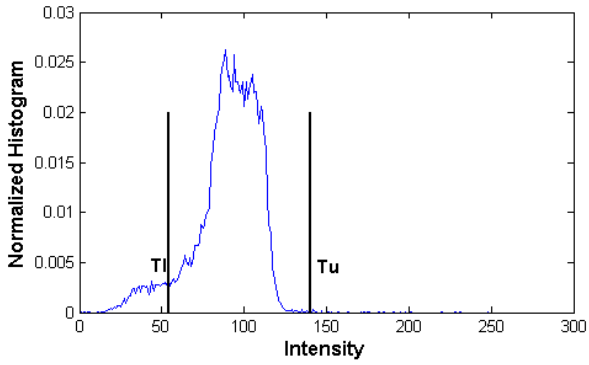

(b)

Fig. 8: (a) The histogram of all templates belong to CASIA V4.0 Lamp left eyes in average. (b) The histogram of the extracted template in Fig. 7(a3) and obtained the upper threshold ($T_u = 140$) and lower threshold ($T_l = 54$) values.

3.5 Iris Classification with Sparse Recovery and PCA

In this paper, the sparse representation and SR for iris segmentation has been used for the first time. Since the SR theory for iris recognition [13] is also used, we need an over-complete dictionary of iris images. It was shown if the number of iris images for each class in the dictionary is 9-10 then the algorithm performance is appropriate [13].

We know that the main advantage of using PCA is reducing the size of multidimensional data while keeping the main features. As mentioned above, for the SR classifier, we need an over-complete dictionary. Using PCA decreases the dictionary size and also keeps the main features of dictionary elements. Obviously, smaller size dictionary means less computation cost and so less running time for classification.

Assume that we have M iris classes and each class consists of N training images. The procedures of making a redundant or over-complete dictionary is shown in Fig. 10 and explained in following:

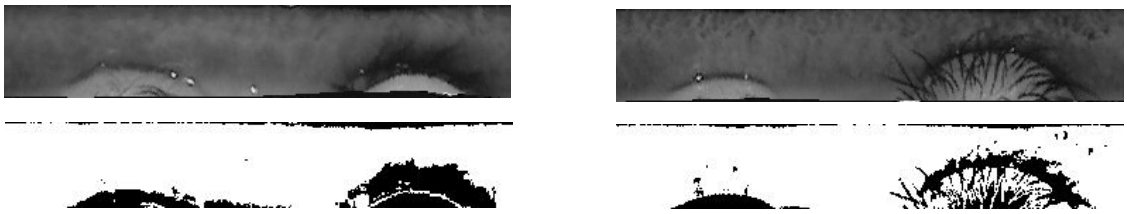

***Fig. 9: Iris templates with their respective masks that is generated by the proposed method. Iris templates in (a) and (b) are respectively the same templates in Fig. 7(a3, b3*).**

1. Use the SPL for pupil localization, segment each iris image individually and extract the iris template with size $m \times 2n$.
2. Use the Haar wavelet transform to generate the iris code. Employ CV (vertical coefficients) and CH (horizontal coefficients) and concatenate them together to have the iris code with size $m \times n$. Furthermore, set those CV and CH coefficients greater than zero into 1 and replace others with zero.
3. Vectorize each iris code and consider it as a column for the dictionary. In this way, the dictionary size is $mn \times MN$.
4. Apply PCA on whole iris code dictionary in order to decrease the dictionary size named as $\mathbf{A}$. The new size of dictionary is $m'n' \times MN$, where $m'n' << mn$ and in this paper, $m'n' = mn/10$.
5. Repeat stages 1, 2 and 4 for any unknown input iris image named $\mathbf{y}$.
6. Solve under-determined problem, $\mathbf{y} = \mathbf{Ax} + \mathbf{e}$ by SR algorithm (in this paper, we used Homotopy). The index of largest coefficient of $\mathbf{x}$ refers to the dictionary column, and indicates the true class.

4. Experimental Results

CASIA-IrisV4 is an extension of CASIA-IrisV3 which has three subsets from CASIA-IrisV3: CASIA-Iris-Interval, CASIA-Iris-Lamp, CASIA-Iris-Twins and three new subsets: CASIA-Iris-Distance, CASIA-Iris-Thousand, and CASIA-Iris-Syn. The CASIA V4.0 Lamp iris including 16213 images of 819 classes is known as a standard data set [21]. Furthermore, as shown some samples in Fig. 4, it includes images with deformed iris circle or occluded iris by eyelids and eyelashes. All images size in CASIA V4.0 Lamp are 640×480 pixels. In this work, we cropped and resized images to 61×81 pixels for computation cost efficiency. Because the dark level intensity span is small for CASIA V4.0 Lamp, we set $c = 9$ in Eq. (6).

In general, any recognition system includes feature extraction and classification. In this paper, Haar wavelet is used for feature extraction. The horizontal (CH) and vertical (CV) Haar wavelet coefficients of iris template are converted to a binary code. So, those CH and CV coefficients with the values greater than zero set to 1 and others replaced by zero. By concatenating these codes we make an iris code with size 60×180 (1350 byte) for each iris template.

For recognition, in this paper, the HD classifier and the SR method explained in Section 3.5 are used. Similar to other biometrics, iris images exhibit both required intra-class and undesirable intra-class variation. Robust iris recognition systems are designed by taking both inter-class and intra-class distortions into account.

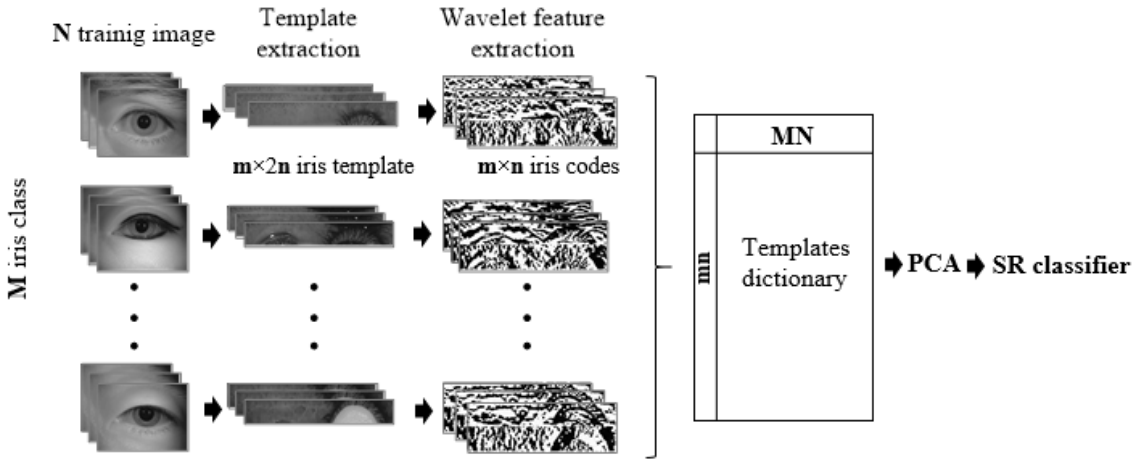

Fig. 10: Full procedures of the proposed method based on SR as a classifier where PCA is used to decrease the dictionary size.

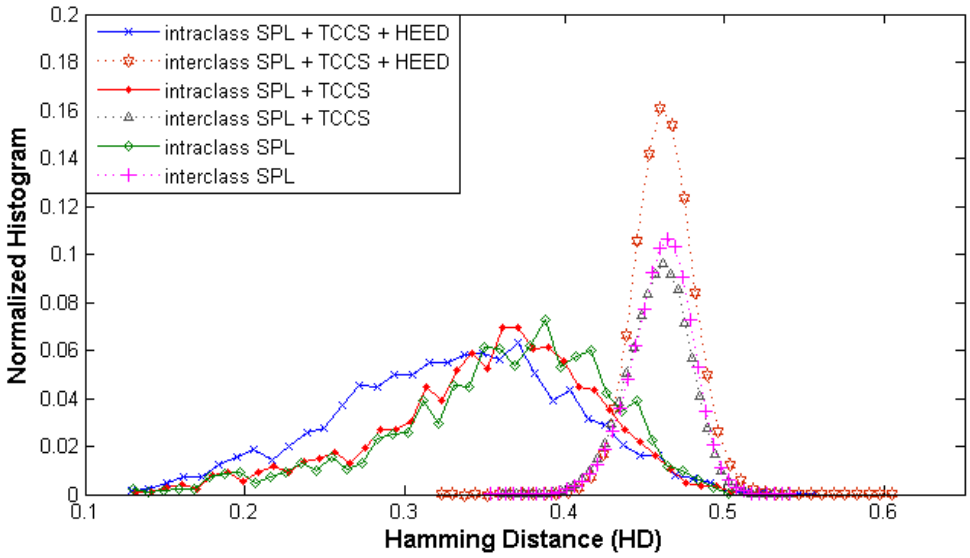

Fig. 11: The HD distributions for inter-class and intra-class of CASIA V4.0 Lamp database.

The HD between two strings of bits is the number of corresponding bit positions that differ in the area of two string masks were common. Using the HD between two bit patterns, a decision can be made as whether the two patterns were generated from the same iris or from different ones. HD can be made using XOR function as:

$$HD = \frac{\left\| (\text{code}A \otimes \text{code}B) \cap \text{mask}A \cap \text{mask}B \right\|_{L1}}{\left\| \text{mask}A \cap \text{mask}B \right\|_{L1}} \tag{10}$$

Where mask$A$ and mask$B$ are the masks of code$A$ and code$B$ respectively. In Fig. 9, obtained sample masks are seen. To evaluate overall performance of the proposed method, we choose randomly 4 left eye images from every class of CASIA V4.0 Lamp, and then measure the intra-class and inter-class HD. Under considering different situations, the HD distributions are shown in Fig. 11. Obviously, using both TCCS and HEED discriminate more between the inter-class and intra-class probes.

In the following, we perform iris recognition procedure to evaluate the overall accuracy of proposed method and compare the HD and SR classifier. In this test, we use

5 left eye images of the first 200 iris classes, then, we randomly choose 2000 probes from the remained images. Therefore, our test dictionary includes 990 samples (because some classes in CASIA V4.0 Lamp is empty such as images of left eye for subject 141) which is stored with 7 different shifts to deal with eye rotation problem. Therefore, the dictionary has 6930 template.

The Receiver Operating Characteristic (ROC) can be obtained by plotting the false recognition rate or false rejection rate (FRR) versus false registered user rejection rate or false acceptance rate (FAR). The FRR is the probability of recognizing any other person than the original one as registered user and the FAR is the probability of wrongly system unrecognized the person whose templates exists in the dictionary.

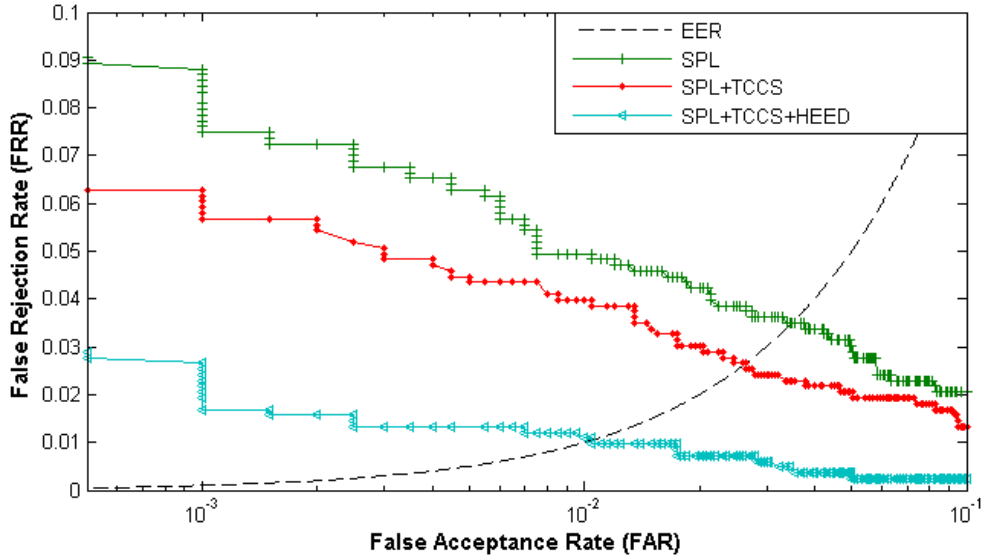

(a)

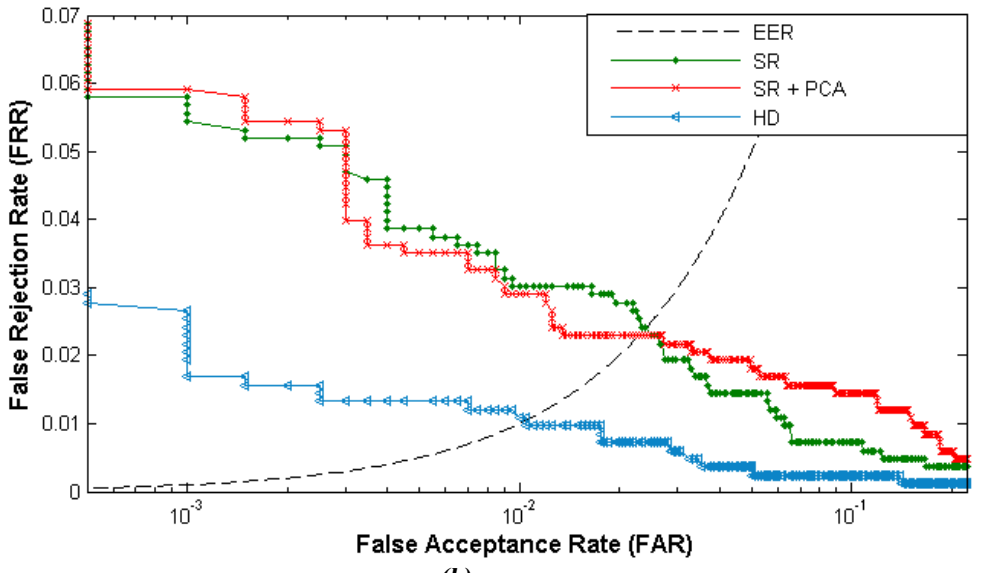

(b)

Fig. 12: (a) ROC curve of the proposed method for CASIA V4.0 Lamp left eyes iris images using HD, (b) comparison the ROC curves by three iris recognition methods.

Table 1: Comparing the achieved accuracy and the segmentation time of the proposed algorithm and other different methods for iris recognition application. The similarity measure was Hamming distance in all methods.

Method	Feature extraction	Accuracy (%)	Segmentation Time (Sec)
Pulling & pushing [3]	Ordinal measure filters	99.25	0.02
OSRIS [22]	Characterizing Key Local Variations	85.11	6.21
Pcode [22]	Characterizing Key Local Variations	71.23	1.96
Weighted Adaptive Hough and Ellipsopolar [22]	Characterizing Key Local Variations	95.64	0.26
The proposed method (SPL+TCCS+HEED)	2-D Haar wavelet	98.95	0.66

The ROC curve of the proposed method is shown in Fig. 12-a by using HD, and the ROC curve based on HD and SR classifier is shown in Fig. 12-b. As, it is seen in Fig. 12-a, the best result achieved by using SPL with masking (TCCS) and contour shifting (HEED) method together. Also, in situation that there is not many training images for each class in the dictionary, the HD performs better than SR algorithm. In addition using PCA for SR classifier increases the recognition rate slightly and decreases the run time of classification but still the HD result is better. Although, the performance of HD is better than SR+PCA, it is time consuming. So, in real time applications, the SR+PCA is preferred. In addition, in order to compare the accuracy of the proposed method with other state of art references, the results of four different algorithms are shown in Table 1. As seen, the achieved result of the proposed method, considering that we used one of the simplest methods for feature extraction (Haar wavelets) in comparison with methods used more complex feature extraction algorithms such as ordinal measures, is acceptable in comparison with other methods in terms of speed and performance though it is not the best.

In order to study the effectiveness of adding TCCS and HEED in segmentation and PCA in classification, further experiment is carried out. The achieved recognition errors on CASIA V4.0 Lamp using HD are %3.5, 2.6, 1.05 when SPL, SPL+TCCS, and SPL+TCCS+HEED are used. In addition, the consuming times for recognition without any claimed identity (the comparison between probe and all dictionary templates) are 1.07, 1.65 and 0.04 seconds whenever HD, SR and SR+PCA are used respectively for classification. The experiment has been done by using Matlab 8.1, on an Intel® Core™ i5-4200M (2.5GHz), 6GB RAM computer.

5. Conclusion

In this paper, a new method based on sparse representation and SR for iris segmentation and pupil localization is proposed. An approach for reducing the noncircular pupil boundary effect that can be used by any circle based iris segmentation algorithm is also introduced. Furthermore, a new method for generating the occlusion mask based on histogram thresholding is proposed where every mask is adaptively generated according to the input template information. The experimental results show that using the generated occlusion mask increases the accuracy of iris recognition rate. We also used the SR for classification whereas PCA employed to have an efficient dictionary size. As a conclusion, the compressive sensing theory can be used in many applications and for different purposes by considering a suitable model.

Acknowledgment

The authors would like to thank the anonymous reviewers who contributed to considerably improve the quality of this paper. Portions of this research use the CASIA V4.0 Lamp database. The authors would like to thank the Chinese Academy of Sciences, Institute of Automation for providing an access to this database.

References

[1] Daugman, J. G. : "Probing the Uniqueness and Randomness of Iris Codes: Results From 200 Billion Iris Pair Comparisons", Proceedings of the IEEE, 2006, 94, (11), pp. 1927–1935.

[2] Daugman, J. G. : "New Methods in Iris Recognition", IEEE Transactions on Systems, Man, and Cybernetics, , 2007, 37, (5), pp. 1167-1175.

[3] He, Z., Tan, T., Sun, Z., Qiu, X. : "Towards Accurate and Fast Iris Segmentation for Iris Biometrics", Pattern Analysis and Machine Intelligence, IEEE Transactions, 2009, 31, (9), pp. 1670-1684.

[4] Daugman, J. G. : "How Iris Recognition Works", IEEE Transactions on Circuits and Systems for Video Technology, 2004, 14, (1), pp. 21-30.

[5] Wildes, R.: "Iris Recognition: An Emerging Biometric Technology", Proceeding of the IEEE, 1997, 85, (9), pp. 1348-1365.

[6] Tisse, C., Martin, L., Torres, L., Robert, M.: "Person identification technique using human iris recognition", Proceedings of Vision Interface, Citeseer, 2002, pp. 294-299.

[7] Liu, X. M., Bowyer, K. W., Flynn, P. J.: "Experiments with an Improved Iris Segmentation Algorithm", Fourth IEEE Workshop on, Automatic Identification Advanced Technologies, 2005, pp. 118-123.

[8] Shah, S., Ross, A.: "Iris Segmentation Using Geodesic Active Contours", IEEE Transactions On Information Forensics and Security, 2009, 4, (4), pp. 824-836.

[9] Kong, W. K., Zhang, D.: "Accurate Iris Segmentation Based on Novel Reflection and Eyelash Detection Model", Proceedings of the IEEE International Symposium on Intelligent Multimedia, Video and Speech Processing, 2001. pp. 263-266.

[10] He, Z., Tan, T., Sun, Z., Qiu, X.: "Robust Eyelid, Eyelash and Shadow Localization for Iris Recognition", IEEE International Conference on, Image Processing, 2008, pp. 265-268.

[11] Candès, E. J.: "Compressive sampling", Proceedings of the International Congress of Mathematicians, 2006, pp. 1433-1452.

[12] Wright, J., Yang, A. Y., Ganesh, A., Sastry, S. S., Ma, y.: "Robust Face Recognition via Sparse Representation", IEEE Transactions on Pattern Analysis and Machine Intelligence, 2009, 31, (2), pp.210-227.

[13] Pillai, J. K., Patel, V. M., Chellapa, R., Ratha, N. K.: "Secure and Robust Iris Recognition Using Random Projections and Sparse Representations", IEEE transactions on pattern analysis and machine intelligence, 2011, 33, (9), pp. 1877-1893.

[14] Chen, S., Donoho, D., Saunders, M.,: "Atomic Decomposition by Basis Pursuit", SIAM journal on scientific computing, 1998, 20, (1), pp. 33-61.

[15] Cand`es, E., Romberg, J., Tao, T.: "Stable signal recovery from incomplete and inaccurate measurements", Communications in Pure and Applied Mathematics, 2006, 59, (8), pp. 1207-1223.

[16] Donoho, D. L., Tsai, Y.: "Fast Solution of L1-norm Minimization Problems When the Solution May be Sparse", IEEE Transactions on Information Theory, 2008, 54, (11), pp. 4789-4812.

[17] Dong, W., Sun, Z.: "Iris Matching Based on Personalized Weight Map", IEEE Transactions on Pattern Analysis and Machine Intelligence, 2011, 33, (9), pp. 1744-1757.

[18] Najafi, M., Ghofrani, S.: "Iris Recognition Based on Using Ridgelet and Curvelet Transform", International Journal of Signal Processing, Image Processing and Pattern Recognition, 2011, 4, (2), pp. 586-597.

[19] Kim, S., Koh, K., Lustig, M., Boyd, S., Gorinevsky, D.: "An interior-point method for large scale L1-regularized least squares", IEEE Journal of Selected Topics in Signal Processing, 2008, 1, (4), pp. 606-617.

[20] Figueiredo, M., Nowak, R., Wright, S.: "Gradient projection for sparse reconstruction: Application to compressed sensing and other inverse problems", IEEE Journal of Selected Topics in Signal Processing, 2011, 1, (4), pp. 586-597.

[21] "CASIA Iris Image Database V4.0", http://www.cbsr.ia.ac.cn/irisdatabase.htm.

[22] Uhl, A., Wild, P.: "Weighted Adaptive Hough and Ellipsopolar Transforms for Real-time Iris Segmentation", Proceedings of the 5th International Conference on Biometrics, 2012, pp.283-290.

[23] Erbilek, M., Fairhurst, M.C.: "Evaluating Iris Segmentation for Scenario Optimisation", 4-th International Conference on Imaging for Crime Detection and Prevention (ICDP), 2011, pp.1-6.

[24] Min, T-H., Park, R-H.: "Eyelid and eyelash detection method in the normalized iris image using", Pattern Recognition Letters, Image/video-based Pattern Analysis and HCI Applications, 2009, 30, (12), pp. 1138-1143.